Rev.Adv.Mater.Sci. 5 (2003) 265-269

ENHANCED REACTIVITY AND PHASE TRANSFORMATION AT THE NANOSCALE: EFFICIENT FORMATION OF ACTIVE SILICA AND DOPED AND METAL SEEDED $TiO_{2-x}N_x$ PHOTOCATALYSTS

James Gole[1], Clemens Burda[2], Andrei Fedorov[1] and Mark White[1]

[1]Schools of Physics and Mechanical and Chemical Engineering, Georgia Institute of Technology, Atlanta, Georgia 30332-0430, USA
[2]Department of Chemistry, Case Western Reserve University, Cleveland, Ohio 44106, USA

Received: June 25, 2003

Abstract. Enhanced reactivity and phase transformation is characterized at the nanoscale. Silica/silicon (SiO_x) nanospheres of diameter ≤ 30 nm generated from equimolar Si/SiO_2 mixtures are found to display enhanced catalytic and reactive properties relative to commonly employed silica support surfaces including fumed silica. This behavior has suggested the possibility of extremely efficient doping and metal seeding involving TiO_2 nanocolloids. The unique reactivity and ready transformation which is found to accompany the facile (seconds) room temperature nitration of TiO_2 nanocolloids, efficiently produces photocatalytically active $TiO_{2-x}N_x$ nanoparticles absorbing light well into the visible region. The introduction of a small quantity of palladium in the form of the chloride or nitrate promotes increased nitrogen uptake, appears to lead to a partial phase transformation, displays a counterion effect (including the acetate), and produces photocatalytic materials absorbing well into the infrared. Additional metal oxides and metals can be used to create doped and seeded materials which can be transformed from liquids to gels facilitating their deposition on surfaces and into porous media. In distinct contrast, attempts to nitride micron-sized TiO_2 particles do not result in the conversion to the oxynitride at room temperature.

An exciting aspect of research at the nanoscale results as nanostructures hold the potential to display an enhanced and unexpected reactivity relative to that at the micron scale and bulk phase. Further, their formation and interaction may be accompanied by phase transformations not commonly observed in bulk systems. We have previously used a modified-flow tube furnace configuration carefully calibrated for temperature, temperature gradients, entrainment gas flow rate, and total pressure, and variable Si/SiO_2 mixtures to generate silica (SiO_x) nanospheres [1,2] in a single step synthesis corresponding to an environmentally benign process versus that for the formation of fumed silica. These nanospheres are found to display enhanced catalytic [3] activity and unexpected reactivity [4]. They can be agglomerated to wire-like configurations subsequently providing a means to grow silica nanotubes [2]. We have also used layered Sn/SnO mixtures to generate SnO_x nanostructures which, at pressures of a few hundred Torr, readily display a phase coexistence between rutile and orthohombic crystal structures [5]. The phase transformation rutile → orthohombic is normally observed at pressures in excess of 150 kbar in the bulk [6]. The efficacy of these processes at the nanoscale has suggested the application of a highly efficient nitriding process [7] to produce $TiO_{2-x}N_x$ nanoparticles which, in distinct contrast for TiO_2, present highly photocatalytically active quantum dots absorbing light well into the visible region. Further, we have simultaneously metal seeded the TiO_2 and $TiO_{2-x}N_x$ nanocolloids. Here we outline the results of our studies of silica and doped titania nanostructures.

Corresponding author: James Gole, e-mail: jim.gole@physics.datech.edu

© 2003 Advanced Study Center Co. Ltd.

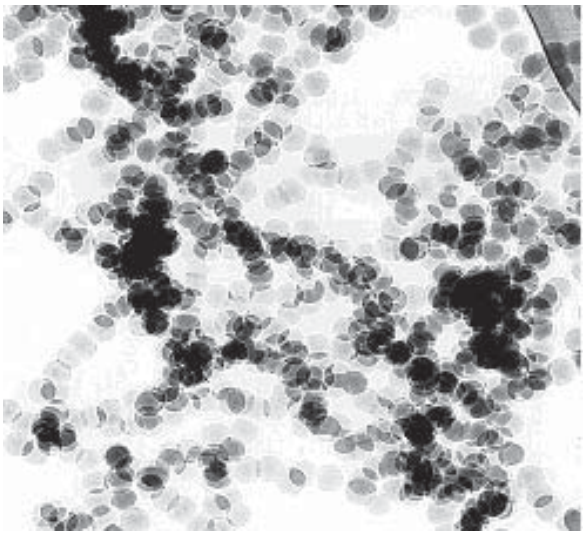

Fig. 1. TEM of virtually 'monodisperse' SiO_2 nanospheres, 30 nm in diameter, synthesized by gas phase condensation from Si/SiO_2.

ACTIVE NANOSTRUCTURED SILICA

Fig. 1 corresponds to a TEM micrograph of dispersed silica (SiO_2) nanospheres of diameter - 30 nm generated in gram quantities on a cold plate placed in the gas flow field of a high temperature synthesis source. Nearly monodisperse particle size distributions for a given experimental run can center on a size between 45 and 8 nm. TEM [1,2], X-ray diffraction [1,2] and ESR [8] measurements demonstrate that the silica nanospheres are amorphous and absent of dangling bonds and defect sites.

The silica nanospheres display some surface properties similar to fumed silica (Cab-O-Sil). They possess silanol groups and have been used as a support for a well-dispersed copper oxide catalyst (formed using the interaction of $Cu(acac)_2$ with the surface silanol groups) and the selective conversion of ethanol to acetaldehyde [3] in a process at least three times more efficient than that using fumed silica.

Heterogeneous catalysts, absorbents, and solid state electronic sensors are derived from either single or multiple metal or metalloid oxides [9]. Their surface oxidation states, obtained usually by a post synthesis treatment, determine, at least in part, their performance [10]. However, we have found that by varying the starting material metalloid/oxide ratio it is possible to prepare highly active SiO_x nanospheres with a desired average surface oxidation state without a post synthesis treatment [4]. The surprisingly facile surface chemistry of these structures versus fumed silica has been evaluated using X-ray photoelectron spectroscopy and the phenol hydroxylation reaction in excess hydrogen peroxide. XPS data reveal a distinctly different Si 2p binding energy, 103.15 eV, for the silica nanospheres (Fig. 1) and Cab-O-Sil, 100.35 eV [4]. When these BE's [11] are compared to the literature values for annealed tetravalent [12], 103.4 eV, and zero valent [12], 99.3 - 99.9, silicon and the nonequilibrium intermediate oxidation states [13] (transition region between Si and SiO_2), + 1 (100.5 - 100.9), and +3 (-103 eV) of surface oxide films [14-17], we are lead to believe that the silicon nanospheres may represent a highly reproducible collection of non-equilibrium phases of silicon and oxygen. The combination of XPS data suggests that the silicon nanospheres show an average silicon oxidation state near +3 and, surprisingly, that the Cab-O-Sil sample shows an average oxidation state perhaps as low as +1. The average Si oxidation states likely arise from a mixture of 0-4 valency in the regions probed by XPS, however, it is established that the regions below and including the top surface layer have been examined [18].

The silicon nanospheres depicted in Fig. 1, generated from an equimolar Si/SiO_2 mix, are considerably more reactive than Cab-O-Sil towards the phenol hydroxylation reaction. This reaction is particularly useful for identifying acid sites [19] and surface oxidation states [20]. The rate constants determined for phenol disappearance given in Table 1, demonstrate that the nanospheres are a factor of eight times more active. While the relative reactivity of silica nanospheres and nanowires (Table 1) generated under similar conditions appears to closely correlate with their surface-to-volume ratio, this is not the case upon comparison with Cab-O-Sil. However, if the silica nanospheres are produced from a mixture, $Si^{4+}(SiO_2)/Si$ = 0.25, they show a lower

Table 1. Phenol Hydroxylation Activity.

Absorbent	*Rate Constant* (*K*, μmol/g-h)
Blank	0.02
Cab-O-Sil	0.56
SnO_x/nanospheres	1.41
SiO_x/nanowires	1.70[a]
SiO_x/nanospheres(1)	4.37[a]
SiO_x/nanospheres(2)	4.87[a]

a. Relative rate constants are closely consistent with surface/volume ratio [4,11].

reactivity comparable to Cab-O-Sil for which XPS indicates a surface oxidation state close to +1 as opposed to +4. These results suggest [4,11] that the silicon surface oxidation state as well as the number of surface silanol groups play important roles in determining the activity of these silicon based solids toward the phenol hydroxylation reaction and that the average surface oxidation state can and must be adjusted to promote reaction. At the nanoscale, with its limited particle dimension relative to the bulk, this adjustment may be more easily accomplished. Further, using the outlined approach, the metalloid oxides are prepared in a two-step generalizable process in the absence of liquid solvents (in the case of fumed silica - HCl from the hydrolysis of silicon tetrachloride), thus offering a more efficient, environmentally friendly, alternate means of adsorbent and catalyst preparation.

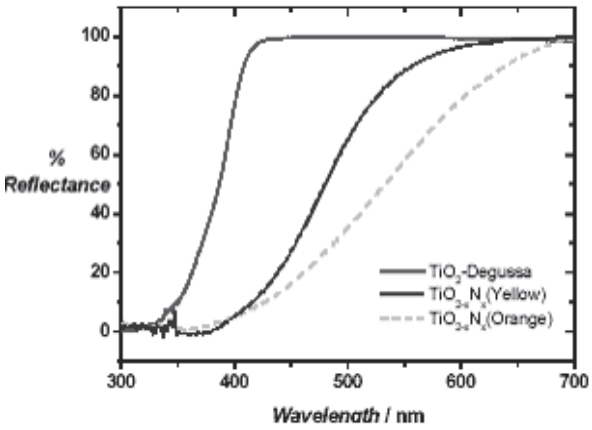

Fig. 2. Reflectance measurements on different TiO_2 samples showing the red-shift effect of nitrogen doping on the absorption of the nanocrystals.

$TiO_{2-x}N_x$ PHOTOCATALYSTS

There has been a long, continued, interest in TiO_2 based photocatalysis [21] because of the relatively high reactivity and chemical stability of the oxide under uv light excitation ($\lambda < 387$ nm) where this energy exceeds the bandgap of anatase (3.2 eV) crystalline n-TiO_2. However, anatase TiO_2 is a poor absorber in the visible region. The cost and accessibility of uv photons make it desirable to develop photocatalysts which are highly reactive under visible light excitation utilizing the solar spectrum or even interior room lighting.

Recently, Asahi *et al.* [22] have prepared $TiO_{2-x}N_x$ films by (1) sputtering TiO_2 targets in an N_2 (40%)/Ar gas mixture and then annealing in N_2 gas at 550 °C for 4 hours and (2) treating anatase TiO_2 powders in an NH_3 (67%)/Ar atmosphere at 600 °C for 3 hours. The nitrogen doping of n-$TiO_{2-x}N_x$ was found to shift the optical absorption and hence photodegredation of methylene blue and gaseous acetaldehyde to the visible region at wavelengths less than 500 nm.

Following the observation of the nanostructure activity which we have previously outlined, we have treated TiO_2 nanocolloids (5-20 nm) [23], directly nitriding with alkyl ammonium salts to produce $TiO_{2-x}N_x$ photocatalysts [24] within seconds at room temperature. Further, by adjusting an initial TiO_2 nanoparticle distribution through careful agglomeration and select metal seeding we produce catalytically active $TiO_{2-x}N_x$ constituencies tuned to absorb well into the visible and near infrared regions.

Fig. 2 compares the optical reflectance spectrum for Degussa P25 TiO_2 (reported at an average size of 30 nm), onsetting sharply at ~ 380 nm, the reflectance spectrum for nitrided, anatase ($TiO_{2-x}N_x$) 3-20 nm nanoparticles, rising sharply at 450 nm, and the corresponding spectrum for nitrided ($TiO_{2-x}N_x$) partially agglomerated nanoparticles, rising sharply at 550 nm. We have also introduced Pd, Ag, and several other metals into a nitriding amine-TiO_2 mixture. XPS analysis [7,24] demonstrates that the introduction of a small quantity of palladium [7] as the chloride or nitrate promotes increased nitrogen uptake. This enhancement is not seen if the palladium is introduced in the form of the acetate. The corresponding reflectance spectra, obtained as palladium incorporation can result in the impregnation of the $TiO_{2-x}N_x$ structure with reduced Pd-based nanocrystallites (primarily for chloride treatment) [7] as well as an apparent phase transformation of a portion of the $TiO_{2-x}N_x$ anatase structure [7], display an even broader optical response extending to considerably longer wavelength, albeit with a lower light absorption efficiency as a function of wavelength. In contrast to this nanoparticle activity, no measurable reaction or heat release is observed as either distinct rutile or anatase TiO_2 micropowders are treated directly with an excess of triethylamine. Further, infrared spectra demonstrate that there is no measurable hydrocarbon incorporation in the nitrided nanocolloids [7].

Photocatalytic activity has been evaluated by measuring the decoloration of methylene blue at 390 and 540 nm, respectively, using a laser producing a 1 KHz pulse train of 120 femtosecond pulses [7,24]. The laser output was used to pump either an optical parametric amplifier to obtain tunable wave-

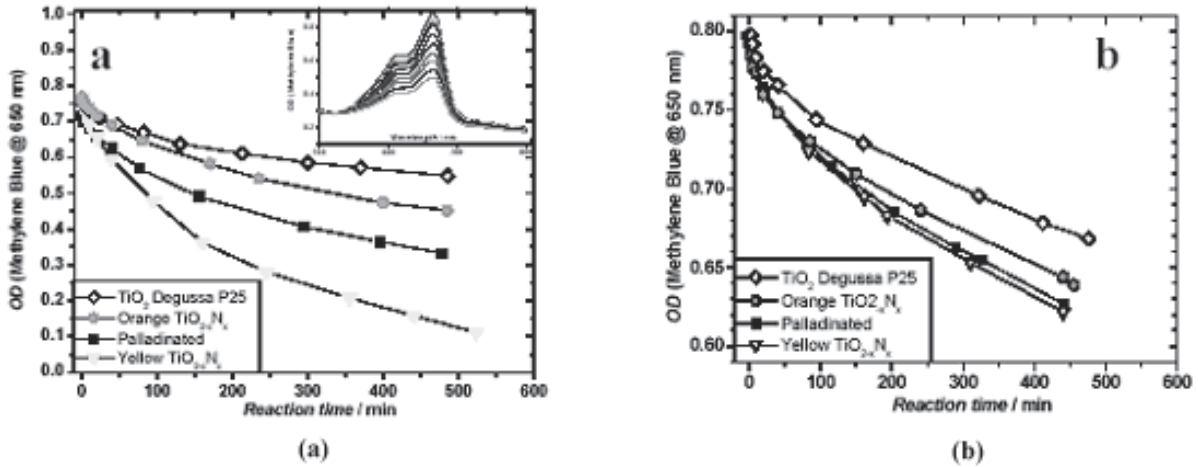

Fig. 3. Comparison of the photocatalytic decomposition of Methylene Blue after (a) 390 nm laser excitation and (b) 540 nm monitored at 650 nm, catalyzed by undoped-TiO_2 (blank test, open diamonds) and Nitrogen-doped TiO_2 nanocrystals. The inset in 3a shows the photodegradation of methylene blue in water at neutral pH.

lengths in the visible spectrum including 540 nm or a second harmonic generation crystal to produce 390 nm photons. Excitation powers were adjusted using a neutral density filter wheel. Fig. 3 demonstrates the photodegredation observed at 390 and 540 nm for methylene blue in water at PH 7. The data for the nitrided samples as well as the palladium treated samples referred to above are consistent with a notable enhanced activity for the $TiO_{2-x}N_x$ constituencies at 390 nm. The comparison of the photocatalytic activity for the palladium treated samples demonstrates a clear counterion effect as the introduction of palladium in the form of the nitrate produces a material whose catalytic activity dominates that of the chloride (Fig. 3). There appears to be little enhanced nitrogen uptake through introduction of the acetate. Preliminary results suggest [7] that the lower activity of the acetate treated sample may result as its introduction promotes the agglomeration of the $TiO_{2-x}N_x$ nanostructures to much larger particles, thus decreasing surface area. While the chloride and nitrate treated samples both maintain the inherent nanostructured composition of the titanium oxynitride, chlorine distributed throughout the nanostructured matrix may furnish a much better trapping site for those electrons liberated through photoexcitation of conduction band electrons.

At 540 nm, all of the nitrided $TiO_{2-x}N_x$ and palladium treated samples still display a notable activity relative to a blank and TiO_2 nanocolloid sample but differences in activity are muted in this less sensitive absorption region [7,24]. In contrast, at wavelengths below 350 nm, the activity of both the TiO_2 and nitrided samples is comparable. Thus nitrided $TiO_{2-x}N_x$ samples which can be generated in several seconds at room temperature are catalytically active at considerably longer wavelength than TiO_2. In preliminary studies, the doped and palladium seeded oxynitrides have also been used to catalyze the oxidation of ethylene to CO_2 and H_2 [25]. These experiments are engineered primarily in a tubular stop-flow reactor as the $TiO_{2-x}N_x$ and Pd - $TiO_{2-x}N_x$ liquidous solutions are transformed to gels facilitating their deposition on surfaces and into porous media. The products of the photocatalyzed oxidation are being sampled with a mass spectrometer system.

The results which we have obtained demonstrate that by forming and adjusting an initial TiO_2 nanoparticle size distribution and mode of nanoparticle treatment, it is possible to tune and extend the absorption of a doped $TiO_{2-x}N_x$ sample well into the visible region. Further, the outlined studies demonstrate that an important modification of a TiO_2 photocatalyst can be made considerably simpler and more efficient by extension to the nanometer regime. The current process can produce submicron agglomerates of a desired visible light absorbing $TiO_{2-x}N_x$ constituency in seconds via a room temperature procedure which otherwise is highly inefficient if not inoperative at the micron scale.

These studies can be expanded. We have also introduced Pt, Ru, Ir, Ni, Co, and Au into both the TiO_2 and nitrided $TiO_{2-x}N_x$ nanocolloid solutions find-

ing distinctly different oxidation state formation, metal ion hydration, and metal particle dispersion, for the doped vs. neat nanocolloids. Further, it also appears possible to extend our approach for substitutional nitration by continuing to operate at the nanoscale. We have now begun to successfully nitride structures of several additional oxides including ZrO_2, HfO_2, SiO_2, and SnO_2.

This paper has attempted to outline examples of interesting and surprising chemistry at the nanoscale. We suggest that future experiments will yield comparable and useful surprises.

REFERENCES

[1] J.L. Gole, J.D. Stout, W.L. Rauch and Z.L. Wang // *Appl. Phys. Lett.* **76** (2000) 2346.

[2] J.L. Gole, Z.L. Wang, Z.R. Dai, J. Stout, R.P. Gao, and Mark White // Polymer Science **281** (2003) 673.

[3] J.L. Gole and M.G. White // *Journal of Catalysis* **204** (2001) 249.

[4] J.L. Gole, B.D. Shinall, A.V. Iretskii, M.G. White, W.B. Carter and A. S. Erickson // *Chem. Phys. Chem*. **4** (2003) 1016.

[5] Z.R. Dai, J.L. Gole, Z.L. Wang and J.D. Stout // *J. Phys. Chem.* **B106** (2001) 1274.

[6] M. Suito, N. Kawai and Y. Masuda // *Mat. Res. Bull.* **10** (1975) 677.

[7] J.L. Gole, C. Burda, *et al.*// *J. Phys. Chem.*, submitted.

[8] S.M. Prokes, W. E. Carlos, J.L. Gole, L. Seals and S. Lewis // *Materials Letters* **54** (2002) 85.

[9] C.N. Satterfield, *Heterogeneous Catalysis* (McGraw-Hill Book Co., 1989).

[10] B.C. Gates, *Catalytic Chemistry* (John Wiley and Sons, Inc. , 1992).

[11] The BE's are calibrated against a gold standard (see Ref. 4) with potential surface charging effects evaluated.

[12] S. Seal, T.L. Barr, S. Krezoski and D. Petring // *Appl. Surf. Sci.* **173** (2000) 339. and S. Ishidzuka, Y. Igari, H. Range and I. Kusunoki // *Thin Solid Films* **89** (2000) 376.

[13] F. Yubero, A. Barranco, J.P. Espinos and A.R. Gonzalez-Elipe // *Surf. Sci.* **436** (1999) 202.

[14] *The Physics and Chemistry of SiO_2 and the Si-SiO_2 Interface*, ed. by C.R. Helms and B.E. Deals (Plenum, New York, 1988).

[15] F.G. Bell and L. Ley // *Phys. Rev. B* **37** (1988) 8383.

[16] J.R. Shallenberger // *J. Vac. Sci. Tech. A* **14** (1996) 693.

[17] F.J. Grunthaner, P.J. Grunthaner, R.P.Vasquez, B.F. Lewis and J. Maserjian // *J. Vac. Sci. Tech. A* **16** (1979) 1443.

[18] A thin layer of higher valent silicon, formed due to air exposure, would make only a small contribution to the overall observed oxidation state probed by XPS.

[19] M. Allian, A. Germain, T. Cseri and F. Figueras, *Heterogeneous Catalysis and Fine Chemicals III* (Elsevier Science Publishers, B. V., 1993).

[20] V.F. Shuvalov and A.P. Moravskii // *Doklady Akademii Nauk SSSR* **234** (1977) 1402; G. Centi, S. Perathones and F. Tiffiro // *J. Phys. Chem.* **96** (1992) 96, and. K. Fairweg and H. Debellefontaine // A*ppl. Catal. B. Environ.* **10** (1996) L229.

[21] See for example: A. Fujishima and K. Honda // *Nature* **238** (1972) 37; J.R. Bonton // *Sol. Energy* **57** (1996) 37; S.U.M. Khan and J. Akikusa // *J. Phys. Chem. B* **103** (1999) 7184; O. Khaselev and J.A. Turner // *Science* **280** (1998) 425; S. Licht *et al.* // *J. Phys. Chem.* **104** (2000) 8920; M.R. Hoffman *et al.* // *Chem. Rev.* **95** (1995) 69; *Photocatalytic Purification and Treatment of Water and Air*, ed. by D.S. Ollis and H. Al-Ekabi (Elsevier, Amsterdam,1993).

[22] R. Asahi, T. Morikawa, T. Ohwaki, K. Aoki and Y. Taga // *Science* **293** (2001) 269.

[23] J. L. Gole, S.M. Prokes, W.E. Carlos, C. She and T. Lian // *Nanoparticles* **738** (2003) 239.

[24] C. Burda, Y. Lou, X. Chen, A.C.S. Samia, John Stout and James Gole // *Nano Lett*. **3** (2003) 1049.

[25] S. Kumar, J.L. Gole and A. Fedorov, in preparation.